Est. 1984

ORIENTAL JOURNAL OF CHEMISTRY
An International Open Free Access, Peer Reviewed Research Journal

www.orientjchem.org

ISSN: 0970-020 X
CODEN: OJCHEG
2016, Vol. 32, No. (4):
Pg. 2243-2249

The Effect of Calcination Temperature on Synthesis of B_4C-nano TiB_2 Composite by Co-Precipitation Method

SAEID ABEDINI KHORRAMI[1], HAMID REZA BAHARVANDI[2] and ROSHANAK LOTFI[1]

[1]Department of Chemistry, North Tehran Branch, Islamic Azad University, Tehran, Iran.
[2]Department of Material, Malek Ashtar University of Technology, Tehran, Iran.
*Corresponding author E-mail : s_akhorrami@iau-tnb.ac.ir

http://dx.doi.org/10.13005/ojc/320457

(Received: January 01, 2016; Accepted: March 25, 2016)

ABSTRACT

Titanium diboride is one of the candidate materials for high temperature applications and also for control rod elements in high temperature reactors. This paper presents the experimental data on the composites of B_4C-nano TiB_2 that were synthesized successfully by co-precipitation method at temperatures between 973 and 1523K. Titanium tetraisopropoxide, boron carbide and isopropanol were used as the precursor materials. The phase constitution and microstructure of B_4C-nano TiB_2 during synthesis were investigated. X-ray diffraction (XRD) and scanning electron microscopy (SEM) were used to determine phase and microstructure of TiB_2-B_4C composites. The DTA/DDTA and TG/DTG results improve that the first exothermic reaction is TiO_2 phase and second exothermic reaction takes place at 1523K which is TiB_2 phase.

Keywords: B_4C-nano TiB_2, DTA/DDTA, TG/DTG, XRD.

INTRODUCTION

As one of the hardest materials known, boron carbide ranks third behind diamond and cubic boron nitride. Boron carbide (B_4C) ceramics possesses excellent mechanical and physical properties of good impact and wears resistance, hardness and high melting, excellent resistance to chemical materials as well as high capability for neutron absorption[1-6]. Moreover the low density of B_4C and its high Young's modulus recommend this material for the construction of light-weight armor such as in the helicopter and similar aero-application[7] However, the widespread application of B_4C ceramics has been restricted because of the poor sinterability due to a low self-diffusion coefficient and the low fracture toughness (< 2.2 MPa $m^{1/2}$)[8, 9].

Titanium diboride with high melting point (3498 K), high hardness (25 GPa), low density (4.5 g cm^{-3}), high electrical conductivity (22× 10^6 Ω cm), good thermal conductivity (96 W/mK) and considerable chemical stability is one of the candidate materials for high temperature structural and wear application[10, 11]. Since both B_4C and TiB_2 have high hardness and high melting points as well as chemical stability at elevated temperature, the B_4C-TiB_2 composites were expected to be used for advanced structural materials.

TiB_2 can be prepared by carbothermic reduction of mixed oxides of titanium and boron, reduction of mixed oxides by metals like aluminum, magnesium and silicon, reduction of titanium oxide by boron carbide and carbon or synthesized from the elements by heating, mechanical alloying or self-propagating high temperature synthesis[12-14], pulsed electric current sintering[15], mechanochemical synthesis[16], dc magnetron sputtering[17] and milling assisted sol-gel [18-21].

Being intrinsically brittle, B_4C often requires some additive to improve its mechanically properties and sintering behavior. Numerous researchers have shown that the addition of TiB_2 to B_4C can decrease the porosity level and improve the fracture toughness as well as flexural strength[22]. Recently, some researchers of B_4C based-composites such as B_4C/CrB_2, B_4C/Al, B_4C/TiC and B_4C/ZrB_2 have been carried out[23]. It has been considered that the additions of secondary phases to B_4C matrix can improve its mechanical properties[24].

In the present study, B_4C-nano TiB_2 composites with 10 ww% TiB_2 were obtained by in situ synthesis from boron carbide, titanium tetraisopropoxide and isopropanol. The effect of calcination temperature on the size, morphology and phase were discussed. Titanium diboride was synthesized by co-precipitation method. Also, thermogravimetric study on the formation of TiB_2 by boron carbide reduction of TiO_2 was carried out in our laboratory.

EXPERIMENTAL

Boron carbide (95%, B_4C, Merck), titanium tetraisopropoxide (97%, TTIP, Alfa Aesar), isopropanol (99.6%, Merck) were used to synthesis. All materials were used without further purification, but were dried in an oven at 423K to remove the moisture content before use. Boron carbide contains 5.0 ww% phenolic resin which used as carbon source. Deionized water was used for all experiments. The precursor powders were obtained by using co-precipitation method. TiB_2 was prepared by the reaction given below:

$$2TiO_2 + B_4C + 3C \rightarrow 2TiB_2 + 4CO$$

Titanium tetraisopropoxide (1.15 mol) and boron carbide (18.1 mol) were dissolved in isopropanol (solution A). Also, boron carbide was

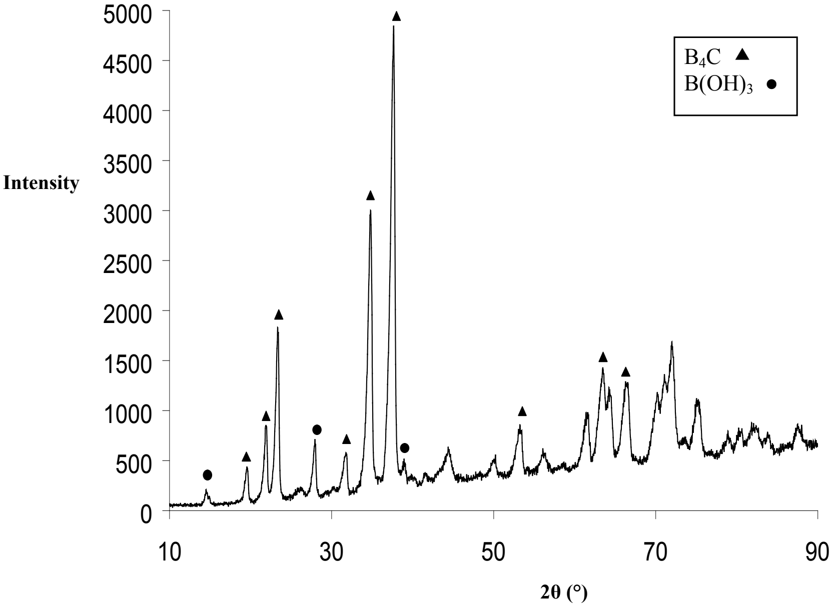

Fig. 1: XRD pattern of initial B_4C

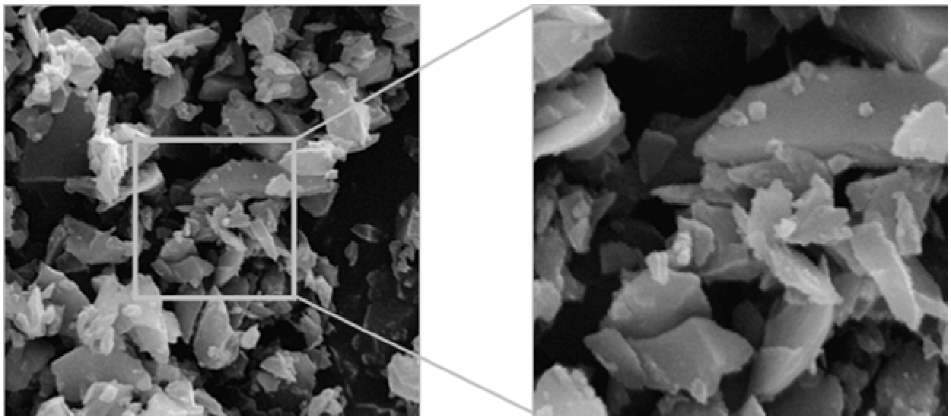

Fig. 2: SEM image of initial B_4C

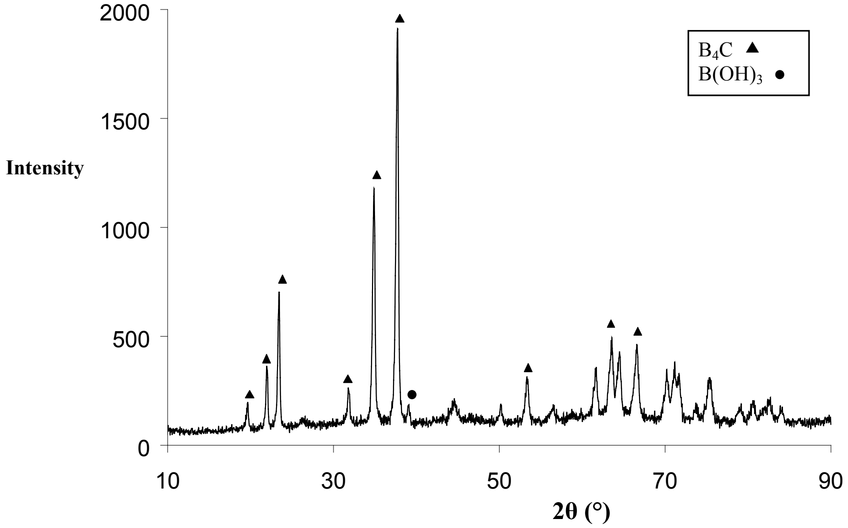

Fig. 3: XRD pattern of the mixture of TTIP, B_4C and isopropanol after milling at about 430K

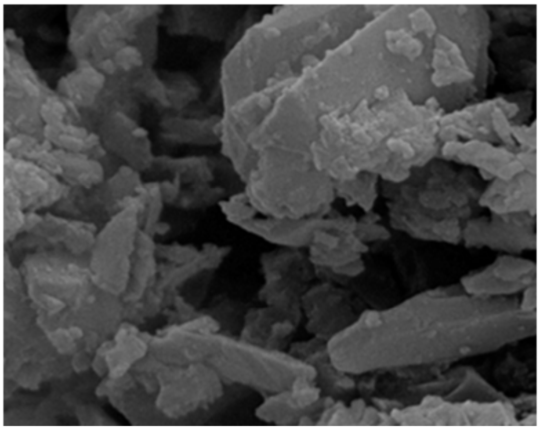

Fig. 4: SEM image of the mixture of TTIP, B_4C and isopropanol after milling at about 430K

dissolved in deionized water and isopropanol (solution B). Solution B was gradually added to solution A. The prepared mixture was stirred and heated at 298K for 4h. In this work, B_4C-nano TiB_2 composites are contained 10 ww% TiB_2.

The X-ray diffraction pattern (XRD, X'Pert MPD, Philips, Holand) and scanning electron microscopy (SEM, XL-30, Philips, Holand) of initial B_4C is shown in Figures 1 and 2, respectively. The crystalline phase during the reaction was investigated by an X-ray diffractometer using Cu-Kα radiation (40 kV, 40 mA). The mixture of TTIP, B_4C and isopropanol was placed at 423-433K.

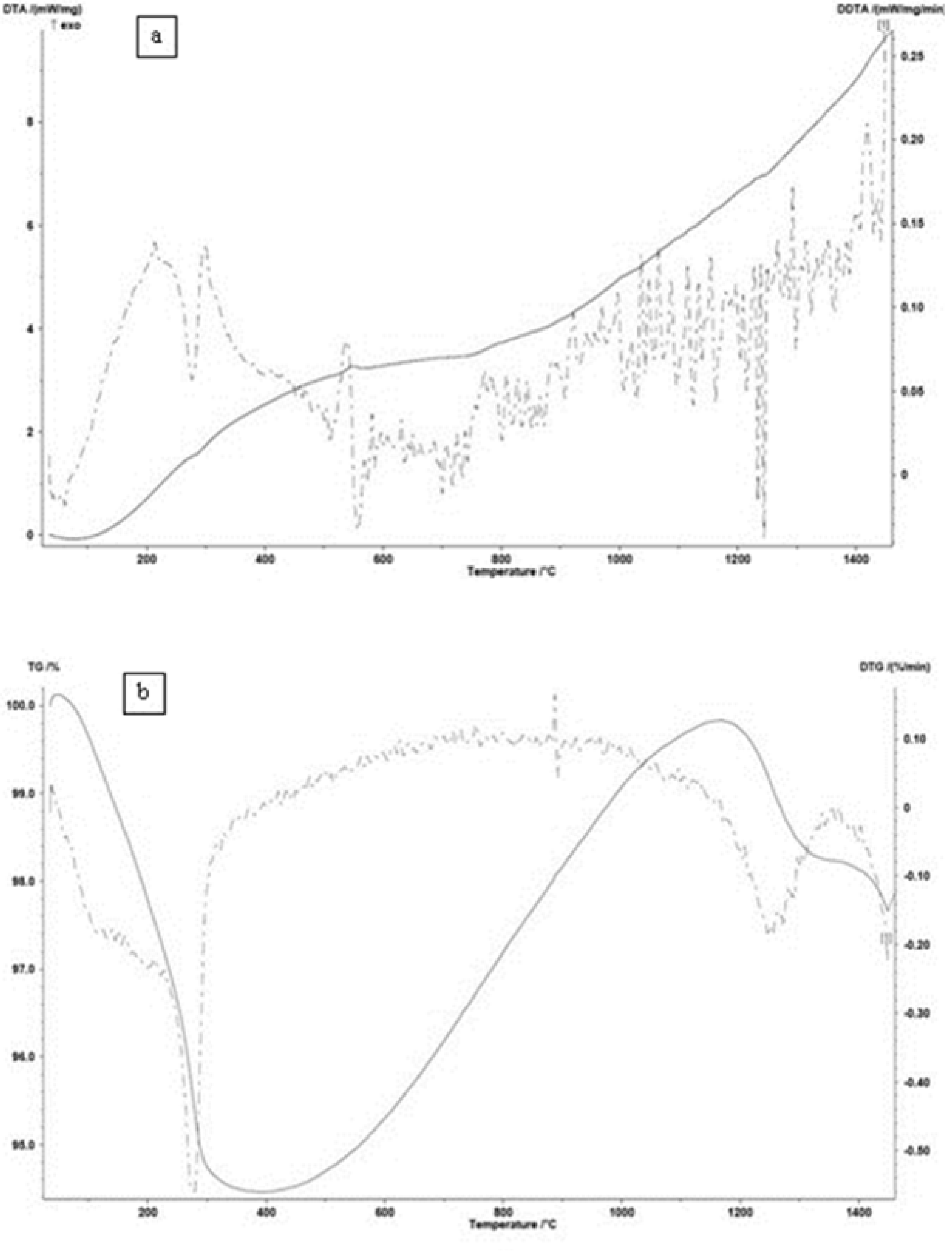

Fig. 5: DTA/DDTA and TG/DTG curves of the formation of titanium diboride for a temperature up to 1700K

Then, the powder were milled and after that, the XRD pattern and SEM were used to determined of particles size and to study of morphology that are illustrated in Figures 3 and 4, respectively. The prepared powder were placed to determine calcination temperature at 973, 1273 and 1523K for 60 minutes with 150 sccm (denotes cubic centimeter per minute at STP) argon flow.

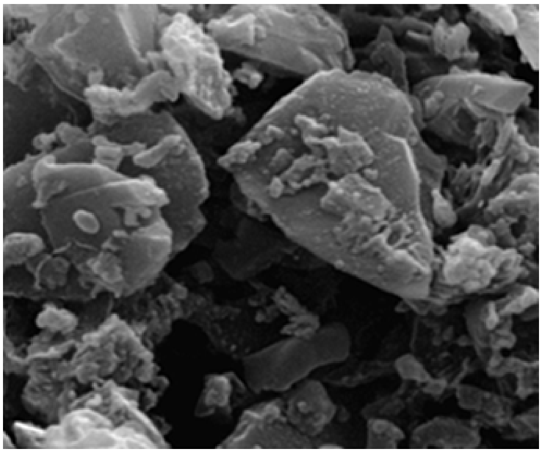

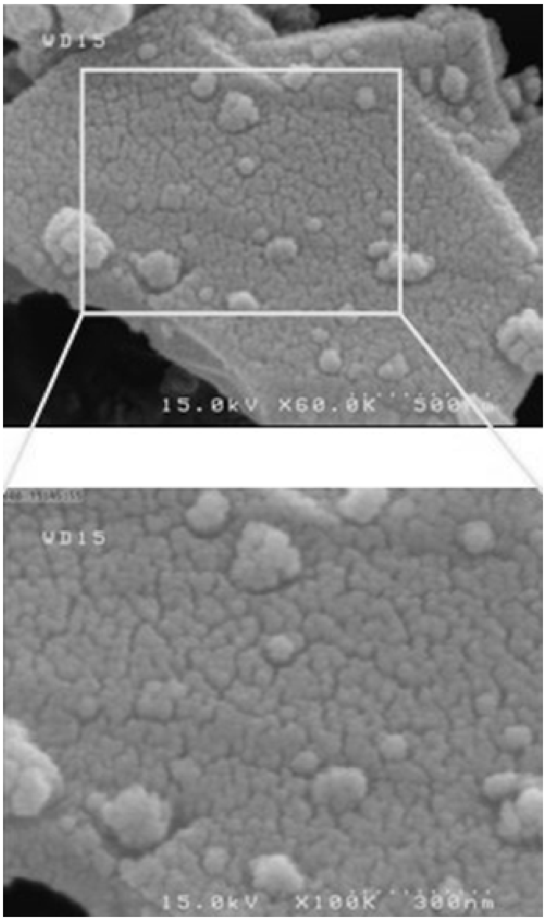

Fig. 6: SEM image of the B_4C-nano TiB_2/TiO_2 composite at: (a) 1273 and (b) 1523K

Figure 5 presents the DTA/DDTA and TG/DTG plots of the formation of titanium diboride.

The composition and nanostructure of the B_4C-TiB_2 composites in 1273 and 1523K were shown by SEM in Figure 6.

Also, XRD patterns of B_4C-TiB_2 composites at 937, 1273 and 1523K for 60 minutes with 10 ww% of TiB_2 are shown in Figure 7 that is used to determined for composites phases.

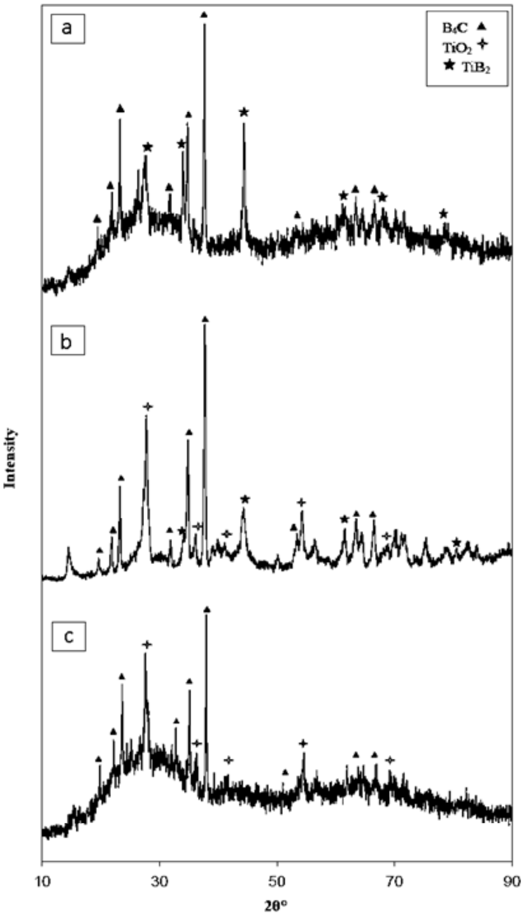

Fig. 7: Diffractographe showing the comparative effects associated at different temperature of introducing the mixture: (a) 973, (b) 1273 and (c) 1523K

RESULTS AND DISCUSSION

The prepared powder for formation of B_4C-nanoTiB_2 composites with 10 ww% TiB_2 are placed to determine calcination temperature at 973, 1273 and 1523K with argon flow. The DTA/DDTA and TG/DTG plots in Figure 5 show that the first exothermic reaction is associated with many weight loss leading to dehydration and evaporation of water from $Ti(OH)_4$ phase and the formation of TiO_2 phase by a decrease in mass of about 13.2 wt% that is given by below reaction:

$$Ti(OH)_4 \rightarrow TiO_2 + 2H_2O$$

second exothermic reaction takes place at 1523K which also in this reaction is associated with weight loss about 4.39 wt% that leading to the formation of TiB_2 nanopowder from TiO_2 particles that is given by:

$$TiO_2 + 0.5\ B_4C + 1.5\ C \rightarrow TiB_2 + 2COR$$

Figure 6(a) shows the SEM image of B_4C-nano TiO_2/TiB_2 composites at 1273K. Particles size at 1273K is between 10-70 nm. FE-SEM image indicate the determination of nanoparticle sizes and morphology of TiB_2 on B_4C at 1523K are shown in Figure 6(b). In the SEM of samples, the distribution of the B_4C and nano TiB_2 was not uniform. The dark elongated grains are B_4C, whereas the bright irregular or equiaxed grains are TiB_2. TiB_2 nanoparticles size at 1523K is between 10-40 nm. Figure 7(a) shows the XRD pattern of composite at 937K. In this calcination temperature exist B_4C and TiO_2 phases that is meaning this temperature is not enough to convert TiO_2 to TiB_2. The XRD pattern of composite at 1273K shows that three phases of B_4C, TiO_2 and TiB_2 exist but calcinations temperature should be increased. Figure 7(c) confirms that only TiB_2 and B_4C phases exist at 1523K that is enough to convert TiO_2 to TiB_2. Pure B_4C-nano TiB_2 phases were detected with no peaks of unreacted TiO_2 and $Ti(OH)_4$, thus indicating the full conversion of reagents into products was achieved according to reaction (3). Therefore, results indicate that synthesis of B_4C-nano TiB_2 from calcinations process of mixed powder is achieved at temperature higher than 1523 K. The XRD patterns of the fractured and the ground surfaces of the composites at 973, 1273 and 1523K are compared in Figure 7. The JCPDS card matching the spectra is 86-1129 for rhombohedral B_4C, 84-1286 for anataze TiO_2 and 85-2083 for hexagonal TiB_2. Since the C source is amorphous carbon black only TiO_2 and B_4C phases were found in the starting powder. The XRD pattern reveals full conversion of TiO_2 to hexagonal TiB_2 after 60 minutes at 1523K. Calcinations process at lower temperature than 1523K contain B_4C, TiO_2 and TiB_2 powders. Decreasing of particles size take place because of suitable selection of optimum calcinations and time for growth of TiB_2 nano particles.

CONCLUSIONS

Titanium diboride was synthesized successfully by co-precipitation method using TTIP, B_4C and isopropanol. In this study, nano TiB_2 particles in three steps produce on microstructure surfaces B_4C at three calcination temperature. In the first reaction, TTIP converted to $Ti(OH)_4$. Then, TiO_2 formed from $Ti(OH)_4$ at 553K. Finally, TiO_2 was transferred TiB_2. The fracture surfaces of the powder were observed by FESEM. The micrographs, reported in Figure 6 confirmed the complete densification of the nanostructured powders. The XRD and SEM results are proved which two phases of B_4C and nano TiB_2 with 10 ww% at 1523K. The nanoparticle sizes of the synthesized nano TiB_2 on surface of B_4C microstructures were found between 10-40 nm.

REFERENCES

1. Chen, M. W.; Mccauley, J. W.; Lasalvia, J. C. *J. American Ceram. Soci.* **2005**, *88*, 1935-1942
2. Roy, T. K.; Subramanian, C.; Suri, A. K. *Ceram. Int.* **2006**, *32*, 227-233
3. Rutkowski, P. *Compos. Theory and Prac.* **2013***, 13,* 33-39
4. Hayun, S.; Rittel, D.; Frage N. *Mater. Sci. Engin. A* **2008**, *487*, 405-409
5. Fanchini, G.; Gupta, V.; Mann, A. B. *J.*

American Ceram. Soci. **2008**, *91*, 2666-2669

6. Srivatsan, T. S.; Guruprasad, G.; Black, D.; Radhakrishnan, R.; Sudarshan, T. S. *Powder Technol,* **2005**, *159*, 161-167.
7. Deng, J.; Sun, J. *Ceram. Int.* **2009**, *35*, 771-778
8. Adrian, G.; Yehoshua, Y.; Ayala, G. *J. Europ. Ceram. Soci.* **2007**, *27*, 695-700
9. Gopal Krishna, U. B.; Sreenivas Rao, K. V.; Vasudev, A. B. *Inter. J. Metallur. & Mater. Sci. and Engin.* **2013**, *3*, 41-48
10. Pezzotta, M.; Zhang, Z. L.; Jensen, M.; Grande, T.; Einarsrud, M. A. *Computational Mater. Sci.* **2008**, *43*, 440–449
11. Licai, F.; Jun, Y.; Qinling, B.; Weimin, L. *Nanoscale Res. Lett.* **2009**, *4*, 11–16
12. Tang, W.; Zheng, Z.; Wu, Y.; Wang, J.; Lu, J.; Liu, J. *Transactions of Nonferrous Met. Soci. of China*. **2006**, *16*, 613-617
13. Deorsoia, F. A.; Atias Adrian, I. C.; Ortigoza Villalba, G. A.; Debenedetti, B. *Mater Research Bull.* **2011**, *46*, 995-999
14. Aminikia, B. *Powder Technol.* **2012**, *232*, 78-86
15. Huang, S. G.; Vanmeensel, K.; Vander Biest, O.; Vleugeis, J. *J. Europ. Ceram. Soci.* **2011**, *31*, 637-644
16. Aviles, M. A.; Cordoba, J. M.; Sayagues, M. J.; Gotor, F. J. *Ceram. Int.* **2011**, *37*, 1895-1904
17. Sanchez, C. M. T.; Rebollo Plata, B.; Maiada Costa, M. E.; Freire, F. L. *Surf. and Coat. Technol.* **2011**, *205*, 3698-3702
18. Rabiezadeh, A.; Ataie, A.; Hadian, A. M. *Int. J. Refractory Metal. and Hard Mater.* **2012**, *33*, 58-64
19. Nemeryuk, A. M.; Lylina, M. M. *Orient. J. Chem.* **2015**, *31*, 2415-2420
20. Glushko, V. N.; Sadovskaya, N. Y.; Usova, O. A.; Blokhina, L. I.; Kozhukhov, V. I. *Orient. J. Chem.* **2015**, *31*, 2515-2520
21. Nemeryuk, A. M.; Lylina, M. M. *Orient. J. Chem.* **2015**, *31*, 2481-2486
22. Lin, Q.; Dong, S.; He, P.; Zhou, H.; Hu, J. *J. Inorganic Mater*. **2015**, *30*, 667-672
23. Hongkang, W.; Yujun, Z.; Xiangyu, D. *J. Ceram. Process Resea.* **2011**, *12*, 599-601
24. Du, B.; Paital, S. R.; Dahotre, N. B. *Optics & Laser Technol.* **2013**, *45*, 647-563.